



Spatial-temporal patterns of PM_{2.5} concentrations for 338 Chinese cities

Wei-Feng Ye ^{a,*}, Zhong-Yu Ma ^{a,b}, Xiu-Zhen Ha ^c



^a School of Environment & Natural Resources, Renmin University of China, Beijing 100872, China

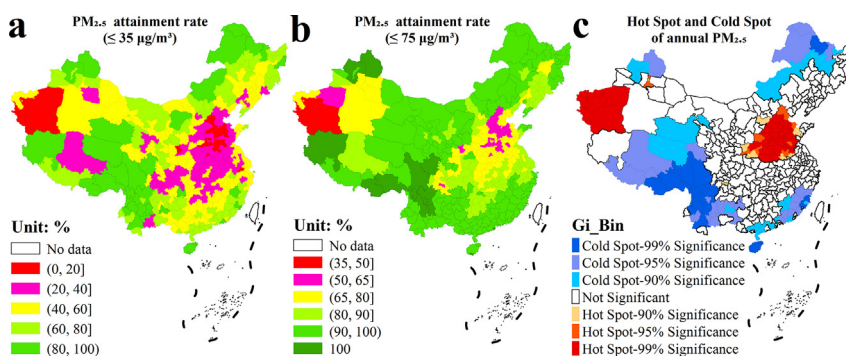
^b State Information Centre, Beijing 100045, China

^c School of Economics, Renmin University of China, Beijing 100872, China

HIGHLIGHTS

- Spatiotemporal patterns of PM_{2.5} in 338 Chinese cities are explored at different time-scales.
- Diurnal variations of PM_{2.5} exhibited a W-shaped trend, while the daily PM_{2.5} presented a U-shape.
- Only 103 cities met the national annual PM_{2.5} standards ($\leq 35 \mu\text{g}/\text{m}^3$) in 2016.
- PM_{2.5} has significant spatial autocorrelation and clustering characteristics.
- Hot spot areas were found in the Beijing-Tianjin-Hebei region and southwest Xinjiang.

GRAPHICAL ABSTRACT



ARTICLE INFO

Article history:

Received 12 December 2017

Received in revised form 5 March 2018

Accepted 6 March 2018

Available online xxxx

Editor: Jianmin Chen

Keywords:

PM_{2.5} concentrations
Spatial-temporal patterns
Spatial autocorrelation
China

ABSTRACT

Air pollution has become a major concern in cities worldwide. The present study explores the spatial-temporal patterns of PM_{2.5} (particles with an aerodynamic diameters $\leq 2.5 \mu\text{m}$) and the variation in the attainment rate (the number of cities attaining the national PM_{2.5} standard each day) at different time-scales based on PM_{2.5} concentrations. One-year of monitoring was conducted in 338 cities at or above the prefectural level in China. Spatial hot spots of PM_{2.5} were analyzed using exploratory spatial data analysis. Meteorological factors affecting PM_{2.5} distributions were analyzed. The results indicate the following: (1) Diurnal variations of PM_{2.5} exhibited a W-shaped trend, with the lowest value observed in the afternoon. The peak concentrations occurred after the ends of the morning and evening rush hours. (2) Out of 338 cities, 235 exceeded the national annual PM_{2.5} standards ($\leq 35 \mu\text{g}/\text{m}^3$), with slightly polluted ($75\text{--}115 \mu\text{g}/\text{m}^3$) cities occupying the greatest proportion. (3) The attainment rate showed an inverted U-shape, while there was a U-shaped pattern observed for daily and monthly mean PM_{2.5}. (4) The spatial distribution of PM_{2.5} concentrations varied greatly, PM_{2.5} has significant spatial autocorrelation and clustering characteristics. Hot spots for pollution were mainly concentrated in the Beijing-Tianjin-Hebei area and neighboring regions, in part because of the large amount of smoke and dust emissions in this region. However, weather factors (temperature, humidity, and wind speed) also had an effect. In addition, southwest Xinjiang experienced heavy PM_{2.5} pollution that was mainly caused by the frequent occurrence of sandstorms, although no significant relationship was observed between PM_{2.5} and meteorological elements in this region.

© 2018 Elsevier B.V. All rights reserved.

* Corresponding author.

E-mail address: plyw08@163.com (W.-F. Ye).

1. Introduction

Air pollution has become a severe threat and challenge in China, especially for PM_{2.5} (particles with an aerodynamic diameter $\leq 2.5 \mu\text{m}$) pollution (Zhang and Cao, 2015). PM_{2.5} is the primary air pollutant in most Chinese cities; among the heavy and severe pollution days in 2016, those with PM_{2.5} as the primary pollutant accounted for 80.3% (MEP, 2017b). Many studies have confirmed that exposure to ambient PM_{2.5} is associated with numerous adverse health effects, including increased mortality, decreased lung and immune function, cardiovascular diseases, respiratory diseases, asthma (Cao et al., 2011; Chen et al., 2017; Ding et al., 2017; Duan et al., 2016; Guo et al., 2009; Hao et al., 2017; Lu et al., 2015). In addition, PM_{2.5} pollution has a detrimental effect on social and economic activity. Haze pollution caused by PM_{2.5} may adversely affect transportation, with delayed or canceled flights and closure of motorways (Li and Zhang, 2014).

In light of this, the Chinese government has amended and enforced the National Ambient Air Quality Standards (GB 3095-2012) and implemented "Atmospheric Pollution Prevention and Control Action Plan" since 2012, with the goal of reducing emissions of PM_{2.5} and other pollutants. Monitoring of PM_{2.5} concentrations was included in the National Ambient Air Quality Standards for the first time. In 2013, the National Ministry of Environmental Protection (MEP) and National Environmental Monitoring Center (NEMC) began monitoring and publicizing hourly and daily air quality monitoring data. This included PM_{2.5} and five other pollutants reported for each monitoring station and each city through the MEP web platform – the National Urban Air Quality Real-Time Publishing Platform (<http://106.37.208.233:20035/>). This website provides adequate information for researchers and decision-makers who need to evaluate and analyze the spatial-temporal distribution and variation in air quality in China.

Although some PM_{2.5} pollution occurs naturally, man-made contamination caused by human activities exacerbates this problem considerably (Mardones and Sanhueza, 2015). Exploring the spatial-temporal distribution of PM_{2.5} concentrations is important for controlling and reducing pollution with effective measures (Hu et al., 2013). With the publication of PM_{2.5} monitoring data, PM_{2.5} pollution has received attention from many researchers in recent years. Past studies investigated the spatio-temporal characteristics of PM_{2.5} using not only natural science methods, such as remote sensing and statistical method, but also studies based on economic or econometric methods and/or models. Commonly published methods include use of geographically weighted regression models (Ma et al., 2014; Wang and Fang, 2016), standard deviation ellipse analysis (Peng et al., 2016), spatial econometric methods (Ma and Zhang, 2014), meta-analysis (Fontes et al., 2017), spatial autocorrelation analysis (Gan et al., 2016; Xu et al., 2017), factor analysis (Xu et al., 2017), and the spatial interpolation method (Wang et al., 2017). Previous studies have evaluated the spatiotemporal patterns of PM_{2.5} pollution in China; the results indicated that PM_{2.5} presents significant spatial differences and clustering patterns and has obvious seasonal variation.

However, previous studies have been limited to provincial capitals or the most important cities of China (Li et al., 2016; Liu et al., 2016; Wang et al., 2014; Wang et al., 2015), the most important regions or provinces (Hu et al., 2014; Xu et al., 2014; Zhou et al., 2016), and the national level (Jin et al., 2017; Li et al., 2017; Peng et al., 2016; Yin et al., 2017). None of the research has involved all cities in China. This occurred primarily because of the following situation: only 161 cities at or above the prefectural level implemented PM_{2.5} concentration monitoring before 2015. Starting in Jan 2015, all 338 cities in China at the prefectural level or above began to monitor PM_{2.5} concentrations; however, the abovementioned studies were mainly based on PM_{2.5} data obtained prior to 2015. Daily, monthly, and annual variations of PM_{2.5} have received more attention in the literature than studies on the diurnal or hourly variations of PM_{2.5}. In addition, the existing studies mainly

focused on the cities or regions in central and eastern China; cities in western China were included in relatively few studies. Western China has a considerably lower level of economic development and a smaller population size than eastern China, resulting in better air quality. However, enjoying excellent air quality is equally important to all regions and persons, regardless of the level of development. Air quality in western China should also be valued. Therefore, to gain a better and more comprehensive understanding of PM_{2.5} pollution at the city level throughout China in a way that reflects regional and spatial differences, a higher spatial-temporal resolution is necessary (Zhang and Cao, 2015).

For these reasons, this paper analyzes PM_{2.5} monitoring data for 338 cities in China and discusses the spatial-temporal patterns of PM_{2.5} in 2016 using statistical methods and an exploratory spatial data analysis model. Specifically, (1) the temporal variations of hourly, daily, and monthly PM_{2.5} concentrations are explored; (2) the attainment rate (the number of cities attaining national standard in each day and month, and the number of attainment days for each city) of PM_{2.5} are thoroughly discussed; (3) the spatial distributions of monthly and annual PM_{2.5} are illustrated; (4) the spatial autocorrelation and hot spots (HS) of monthly and annual PM_{2.5} concentrations are investigated with exploratory spatial data analysis; and (5) meteorological factors are selected to reveal their relationships with PM_{2.5} concentrations.

2. Materials and methods

2.1. Data sources

Our analysis is based on the monitoring data for 338 cities at the prefectural level or above in China in 2016 (excluding Hong Kong, Macau, and Taiwan due to a lack of accessible data). All these cities have constructed state-level air quality monitoring stations. The monitoring stations have been designated in a mix of urban and background sites, with most of them in urban areas, and a few in the suburbs and rural areas. At each station, automated monitoring systems were installed and used to measure the concentrations of SO₂, NO₂, O₃, and CO according to the National Environmental Protection Standards known as HJ 193-2013 (MEP, 2013b), and PM_{2.5} and PM₁₀ according to HJ 655-2013 (MEP, 2013a). Detailed information about these cities and stations is available from the National Urban Air Quality Real-Time Publishing Platform (NUAQRPP) (<http://106.37.208.233:20035/>).

In January 2013, the MEP of China started publishing real-time hourly and daily concentrations of six pollutants including PM_{2.5}, PM₁₀, CO, SO₂, NO₂ and O₃ through the NUAQRPP. The PM_{2.5} data used in the present study was obtained from the NUAQRPP for the period of Jan 1, 2016 to Dec 31, 2016. Then, the monthly, and annual mean concentrations of each city were calculated based on hourly and daily data.

2.2. Exploratory spatial data analysis

Exploratory Spatial Data Analysis is a collection of techniques used to describe and visualize spatial distributions; identify atypical locations or spatial outliers; discover patterns of spatial association, clusters, or HSs; it is also used to suggest spatial regimes or other forms of spatial heterogeneity (Haining, 1990). In practical application, both global and local spatial autocorrelation (or spatial HS analysis) are often adopted to investigate the spatial characteristics of observations.

2.2.1. Global spatial autocorrelation

Global spatial autocorrelation analysis is mainly concerned with the correlation among observations in spatial proximity (Anselin, 1988). Global Moran's I, which was first proposed by Moran (1948), is the most widely known and used statistic to test for the presence of spatial

dependence in observations. The Moran's I can be calculated using Eq. (1):

$$I = \frac{\sum_{i=1}^n \sum_{j=1}^n w_{ij}(x_i - \bar{x})(x_j - \bar{x})}{\frac{1}{n} \sum_{i=1}^n (x_i - \bar{x})^2 * \sum_{i=1}^n \sum_{j=1}^n w_{ij}} \quad (1)$$

where $\bar{x} = \frac{1}{n} \sum_{i=1}^n x_i$; n is the number of spatial units (in this study, $n = 338$); x_i and x_j are the observations of spatial units i and j , respectively; w_{ij} is an element of the spatial weight matrix W which describes the spatial arrangement of all the spatial units in the sample, where $w_{ij} = 1$ if spatial units i and j share a common border and $w_{ij} = 0$ otherwise. Values of Global Moran's I range from -1 to 1 ; a positive (or negative) correlation exists among the observations if $0 < I < 1$ (or $-1 < I < 0$), and the observations are distributed randomly (no correlation) in the space if I is close to or equals 0.

The significance of Global Moran's I is usually measured by the standardized statistic Z as shown in Eq. (2):

$$Z(I) = \frac{I - E(I)}{\sqrt{\text{Var}(I)}} \quad (2)$$

where $E(I)$ and $\text{Var}(I)$ are the expected value and variance of Moran's I, respectively; The methods used to calculate them are listed in the Supplementary Materials.

2.2.2. Hot spot (Getis-Ord G_i^*) analysis

Getis-Ord G_i^* is a tool or technique for cluster analysis which identifies statistically significant spatial clusters of high (HSs) and low (CSs) values (Getis and Ord, 1992; Ord and Getis, 1995). The G_i^* statistic

is calculated using Eq. (3):

$$G_i^* = \frac{\sum_{j=1}^n w_{ij}(x_j - \bar{x})}{\sqrt{\frac{1}{n} \sum_{j=1}^n x_j^2 - \bar{x}^2} \cdot \sqrt{\frac{n}{n-1} \sum_{j=1}^n w_{ij}^2 - \frac{n}{n-1} \left(\sum_{j=1}^n w_{ij} \right)^2}} \quad (3)$$

where $\bar{x} = \frac{1}{n} \sum_{j=1}^n x_j$, while n and w_{ij} are the same as above.

The output of the G_i^* statistic is a Z-score, p-value and confidence level bin (G_i _Bin) for each feature. The Z-scores and p-values are measures of statistical significance. A high positive (or low negative) Z-score and small p-value for a feature indicates a spatial clustering of high (HSs) and low (CSs) values, respectively. The larger (or smaller) the Z-score is, the more intense the clustering of high (or low) values. A Z-score near zero indicates no apparent spatial clustering. The G_i _Bin field also identifies statistically significant HS and CS. Features in the ± 3 , ± 2 and ± 1 bins reflect statistical significance with a 99%, 95% and 90% confidence levels, respectively; and the features in bin 0 is not statistically significant.

3. Results

3.1. Overview of $PM_{2.5}$ concentrations

3.1.1. Diurnal variations of $PM_{2.5}$

Diurnal variations of $PM_{2.5}$ presented a similar W-shaped trend in different months (Fig. 1a). The peak concentrations appeared around 10:00 and 23:00, while the valley values appeared around 6:00 and 16:00. The $PM_{2.5}$ concentration increased from the valley to peak values during the morning and evening rush hour, respectively. $PM_{2.5}$ peaked after the rush hour ended, and then gradually declined, which forms a periodic variation of initially descending and then ascending twice in a single day. The peak values during daytime were greater than that during night from Mar to Sep (non-heating season), while the reverse was

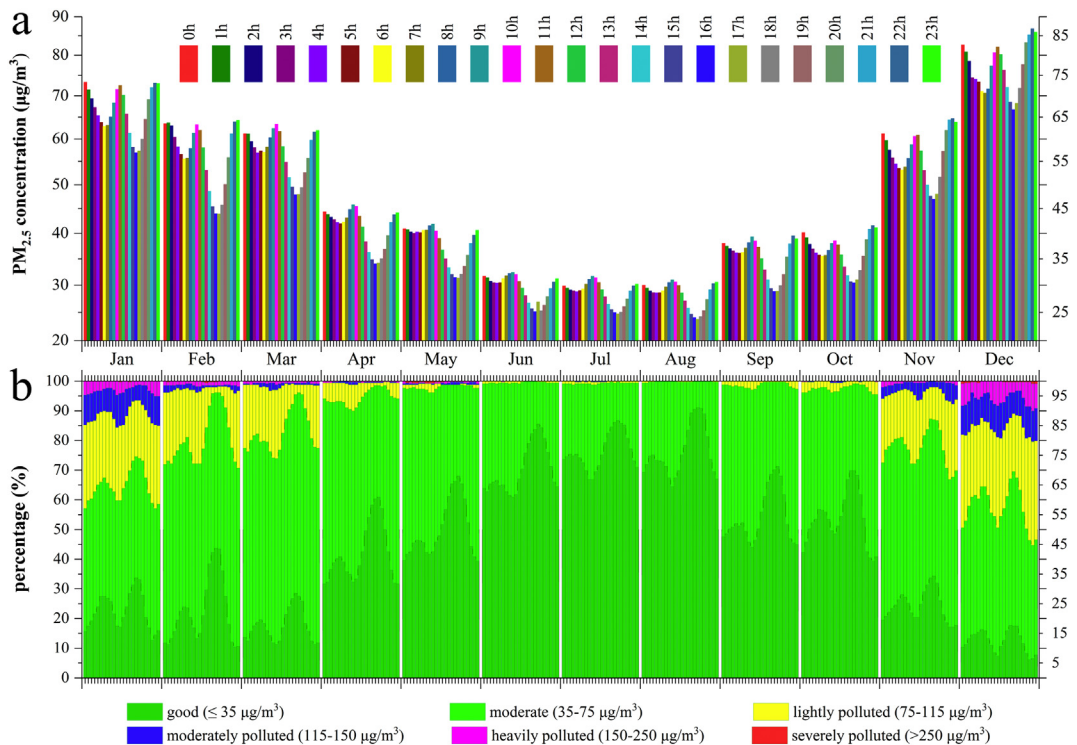


Fig. 1. Diurnal variation of $PM_{2.5}$ (particles with an aerodynamic diameters $\leq 2.5 \mu\text{m}$) concentrations for 338 cities in 2016: (a) diurnal variation of $PM_{2.5}$ in each month. (b) hourly distribution of different $PM_{2.5}$ pollution levels for 338 cities in each month.

true in the other months of the year (heating season). PM_{2.5} concentrations reached the lowest values around 16:00 each day. Valley values appeared around 7:00 in Jan, Feb and Dec (wintertime) and around 4:00 from May to Aug (summertime). Specifically, a time delay for the first valley value varied for a specific day in different seasons. In addition, a time difference was observed in terms of the appearance of peaks among different seasons.

Based on the Technical Regulation on Ambient Air Quality Index of China currently being tried (MEP, 2012), the PM_{2.5} concentration or pollution level is divided into six grades: good ($\leq 35 \mu\text{g}/\text{m}^3$), moderate ($35\text{--}75 \mu\text{g}/\text{m}^3$), as well as slightly ($75\text{--}115 \mu\text{g}/\text{m}^3$), moderately ($115\text{--}150 \mu\text{g}/\text{m}^3$), heavily ($150\text{--}250 \mu\text{g}/\text{m}^3$), and severely ($>250 \mu\text{g}/\text{m}^3$) polluted, respectively. Using this outline, “attainment” means that the hourly or daily PM_{2.5} concentration of a city cannot exceed $75 \mu\text{g}/\text{m}^3$; if it is larger than this limit, the air quality is in non-attainment status or over the standard. The attainment rate (hereinafter “AR”) showed a reverse trend when compared with the variation in concentrations, where PM_{2.5} reached a valley value while AR increased to a peak, and vice versa (Fig. 1b). The proportion of cities with hourly PM_{2.5} $\leq 35 \mu\text{g}/\text{m}^3$ peaked at around 16:00 each day, while PM_{2.5} declined to its lowest value at 16:00.

3.1.2. Spatio-temporal variations of daily and monthly PM_{2.5}

From the perspective of temporal variations, the daily mean PM_{2.5} concentrations of all cities, which ranged from 20.21 ± 13.63 (in Jul 1) to $131.31 \pm 113 \mu\text{g}/\text{m}^3$ (in Dec 19) in 2016 (Fig. 2a), presented a U-shaped pattern of variation. The number of days with daily mean PM_{2.5} attaining the national 24-h standard ($\leq 75 \mu\text{g}/\text{m}^3$) reached 339 days, of which all the 244 days during Apr to Oct met the 24-h limit; meanwhile, 139 days met the national annual standard ($\leq 35 \mu\text{g}/\text{m}^3$). With the change of daily mean PM_{2.5}, the monthly mean PM_{2.5} of all cities also presented a U-shaped trend (Fig. 2a). The average concentration of PM_{2.5} for 338 cities was largest in Dec, and lowest in Aug (Table 1). The monthly mean PM_{2.5} of all cities reached the annual standard during Jun to Aug, and exceeded the limit in the other nine months.

The AR for each day showed an inverted U-shaped pattern (Fig. 2b), where the number of attainment cities for each calendar day initially increased overall and then descended during the year. AR was 100%, 90–100% (<100%), 80–90%, 70–80%, 60–70%, 50–60%, and lower than 50% for nine, 206, 44, 38, 39, 19, and 11 days, respectively. In addition, among the cities with non-attainment of daily PM_{2.5} targets, the largest proportion were slightly polluted, followed by moderately and heavily polluted level (Fig. 2b). More importantly, severely polluted cities

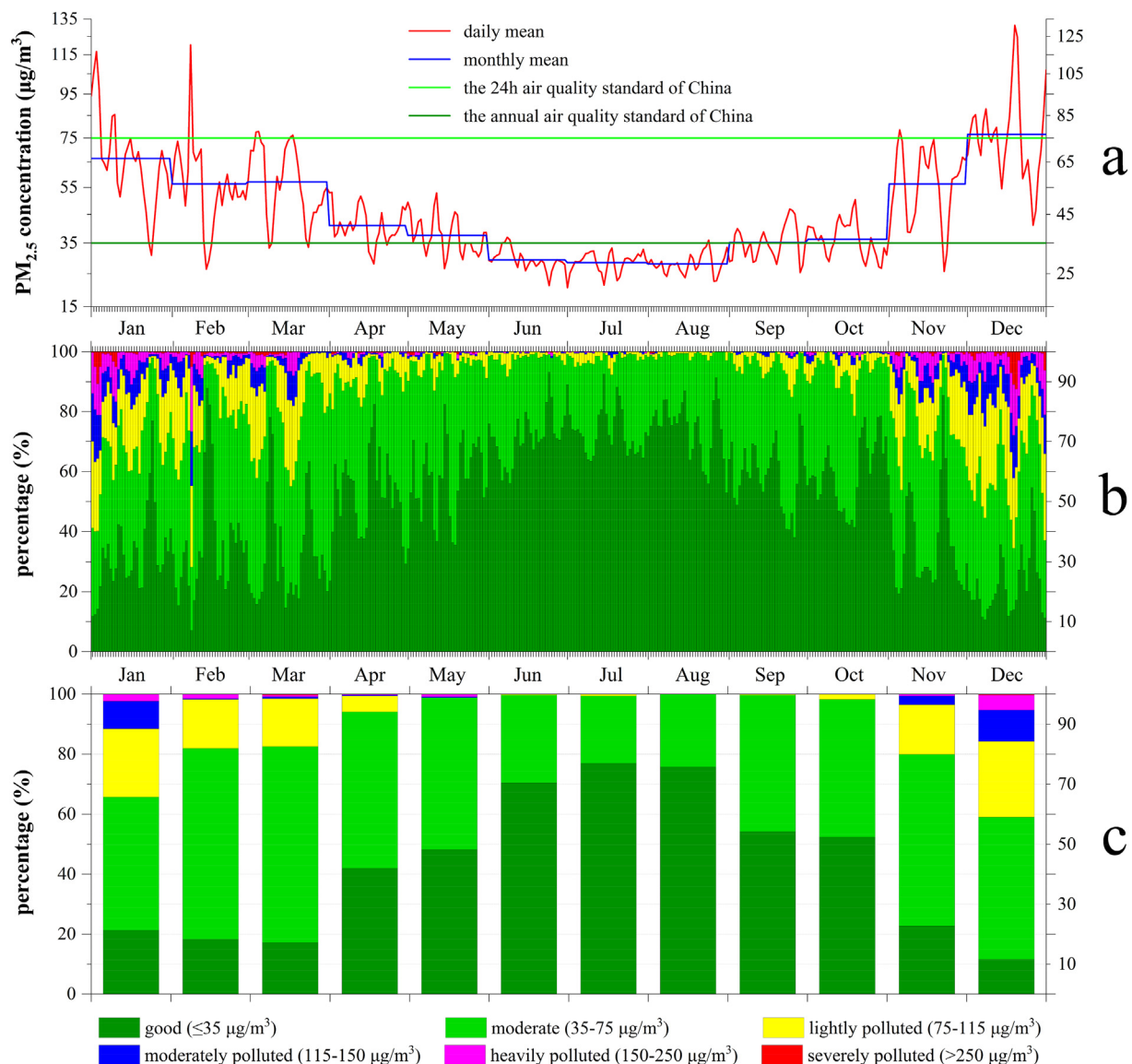


Fig. 2. The temporal variation of PM_{2.5} (particles with an aerodynamic diameters $\leq 2.5 \mu\text{m}$) concentrations for 338 cities in 2016: (a) the temporal variation of daily and monthly mean PM_{2.5}; (b) the daily distribution of different PM_{2.5} pollution levels for 338 cities; and (c) The monthly distribution of different PM_{2.5} pollution levels for 338 cities.

Table 1

Descriptive statistics of PM_{2.5} (particles with an aerodynamic diameters $\leq 2.5 \mu\text{m}$) concentrations for 338 cities in 2016 (Unit: $\mu\text{g}/\text{m}^3$).

Period	Minimum		Maximum		Median	Mean	Standard deviation
	PM _{2.5}	City name	PM _{2.5}	City name			
Jan	11.13	Nyingchi	192.55	Wujiaku	61.18	66.41	35.66
Feb	11.52	Nyingchi	225.69	Wujiaku	52.79	56.38	26.66
Mar	11.29	Altay	510.58	Kashgar	53.73	57.12	34.03
Apr	6.93	Altay	164.70	Kashgar	37.78	41.01	18.46
May	6.97	Altay	224.46	Kashgar	35.63	37.64	20.28
Jun	5.90	Yichun	88.33	Hotan	28.58	29.48	12.49
Jul	5.65	Yichun	102.35	Hotan	26.73	28.53	13.08
Aug	4.97	Yichun	63.19	Aksu	27.45	28.16	9.69
Sep	6.13	Nyingchi	81.20	Shijiazhuang	33.87	35.17	14.02
Oct	8.39	Altay	111.29	Shijiazhuang	34.32	36.28	14.71
Nov	11.23	Sanya	172.10	Linfen	51.90	56.31	27.33
Dec	13.23	Deqen	252.10	Shijiazhuang	69.45	76.60	39.43
Annual	10.28	Altay	157.01	Kashgar	43.72	45.75	18.21

(PM_{2.5} $> 250 \mu\text{g}/\text{m}^3$) should not be neglected; their proportion was higher than 5% on several days and exceeded 10% of all cities on three days (Jan 3, Dec 19, and 20; Fig. 2b). The number of cities with monthly PM_{2.5} $\leq 35 \mu\text{g}/\text{m}^3$ ranged from 39 to 260 in 2016. The AR peaked in Jul (77%), and was lowest in Dec at 12% (Fig. 2c).

Based on the annual limit ($\leq 35 \mu\text{g}/\text{m}^3$; Fig. 3a), the AR (the proportion of attainment days in the year for a city) was lowest (6%) for Aksu Prefecture in southwest Xinjiang Province and was largest

(99.7%) for Lijiang and Deqen in northwest Yunnan Province (Fig. S1 graphically illustrates the location of Chinese provinces). The cities with AR $>80\%$ were mainly distributed in southwest and northeast China, as well as several cities in Xinjiang and Qinghai. Meanwhile, the cities with AR $<40\%$ were mainly in the Beijing-Tianjin-Hebei (BTH) region, eastern China, as well as in southwest Xinjiang. In particular, AR was $<20\%$, 20–40%, 40–60%, 60–80%, and higher than 80% for 22, 92, 114, 75, and 35 cities, respectively.

The AR is based on a 24-h limit ($\leq 75 \mu\text{g}/\text{m}^3$; Fig. 3b); the number of cities where the AR was at high level increased significantly, and the distribution range of cities with low AR was shrinking. Only two regions – Kashgar and Hotan, located in southwestern Xinjiang – had an AR $<50\%$, at 37% for the former and 48% for the latter. The AR was 50–65%, 65–80%, 80–90%, 90–100% ($<100\%$), and 100% for 21, 77, 81, 142, and 15 cities, respectively. Those with 100% ARs were mainly in Yunnan, Sichuan, Tibet, and Xinjiang, implying that PM_{2.5} concentration met 24-h standard in each day of the year for these cities. Furthermore, from Fig. 3a and Fig. 3b, three cities (Kashgar, Hotan and Aksu) with lowest AR and two cities (Altay and Qoqek) with highest AR were all located in Xinjiang. This suggests that northwest Xinjiang is one of regions where PM_{2.5} concentration and air quality are significantly lower than the national limit ($\leq 35 \mu\text{g}/\text{m}^3$), and southwest Xinjiang is one of regions where PM_{2.5} frequently and severely exceeds the national standard.

The distribution of the monthly mean PM_{2.5} in 22 cities met the annual limit in all months of the year; most of these were located in south and southwestern China (Fig. 3d). Meanwhile, 36 cities had a monthly PM_{2.5} exceeding the annual limit in each month of the year; these

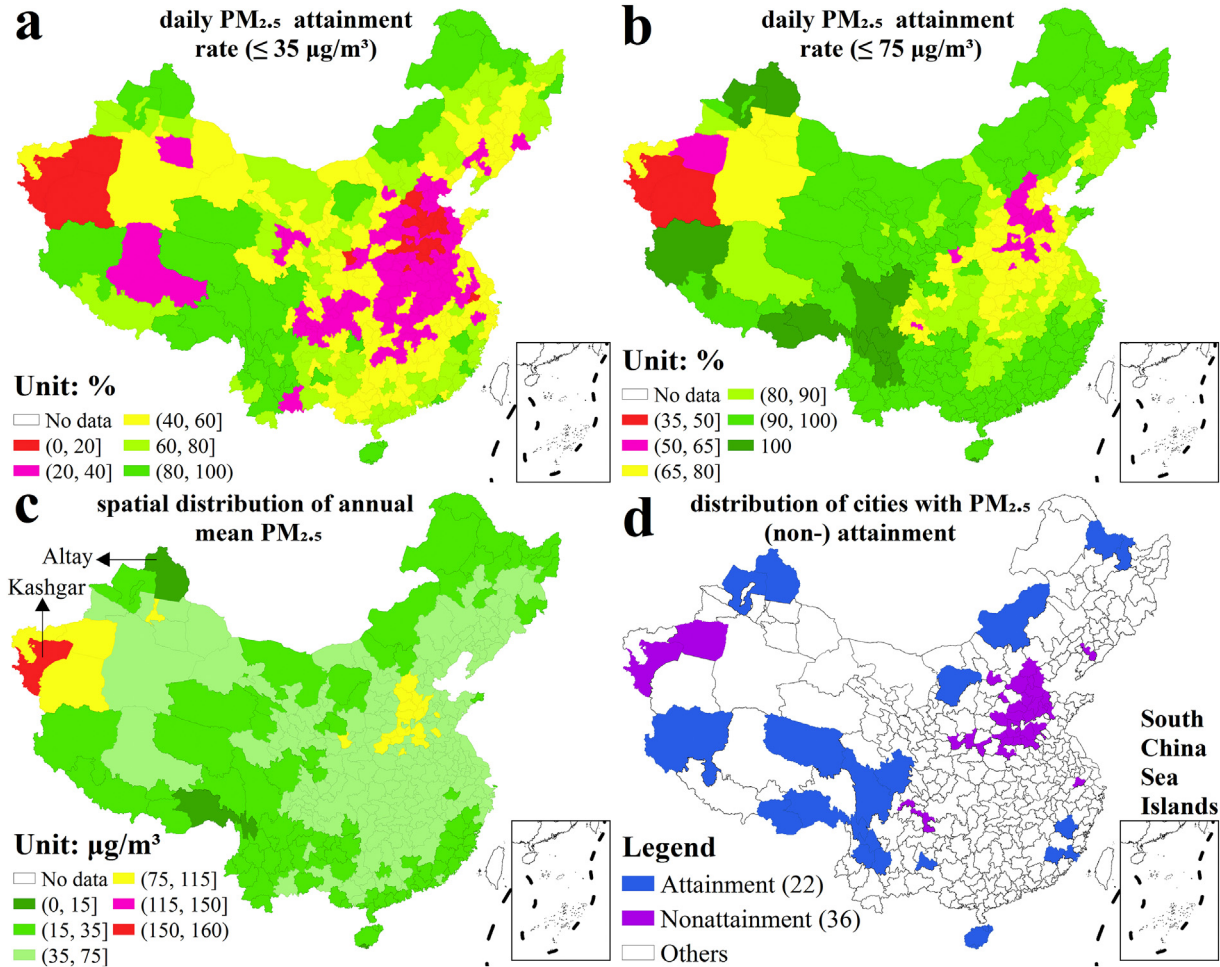


Fig. 3. The spatial distribution of the PM_{2.5} (particles with an aerodynamic diameters $\leq 2.5 \mu\text{m}$) pollution control attainment rate (a and b) and PM_{2.5} concentrations (c). (d) The spatial distribution of cities with PM_{2.5} meeting and not meeting the national standard. "Attainment" and "Nonattainment" indicates cities with PM_{2.5} concentration meeting and not meeting the national annual standard ($35 \mu\text{g}/\text{m}^3$) in all the months of the year; "Others" refers to any other circumstances except for the two above-mentioned circumstances.

were mainly in southwestern Xinjiang, the BTH region and to the south, and in several other provinces.

3.1.3. Spatial distribution of annual PM_{2.5}

The annual PM_{2.5} fell in the range of 10.28 (in Altay) to 157.01 µg/m³ (in Kashgar) with an annual average of 45.75 ± 18.21 µg/m³, exceeding the national Grade II limit ($\leq 35 \mu\text{g}/\text{m}^3$). A total of 103 cities having an annual mean PM_{2.5} meeting Grade II were mainly in northeast, southwest, and southeast China (Fig. 3c). Only four cities had an annual PM_{2.5} reaching Grade I ($\leq 15 \mu\text{g}/\text{m}^3$), including Altay, Deqen, Nyingchi, and Sanya. A total of 211 cities having an annual PM_{2.5} of 35–75 µg/m³ were mainly in west, central-south, east, and northeast China. In addition, 23 cities with annual PM_{2.5} of 75–115 µg/m³ were mainly in central-south Hebei, western Shandong, and northeast Henan. Only one city (Kashgar) had an annual PM_{2.5} > 150 µg/m³.

In addition, it is worth noting that two cities, Altay and Kashgar, recorded the lowest and highest annual PM_{2.5}, respectively; these are all located in Xinjiang, Altay in the northwest and Kashgar in the southwest (Fig. 3c). Fig. S2 illustrates the variation of daily and monthly PM_{2.5} in Kashgar and Altay in 2016. For Kashgar, the daily PM_{2.5} ranged from 11 to 1771 µg/m³ in 2016. Kashgar had 64 days with PM_{2.5} ≤ 35 µg/m³ and 72 days with PM_{2.5} of 35–75 µg/m³; thus the AR was only 37% in 2016. Kashgar also had 72, 49, 68, and 41 days with PM_{2.5} at the slightly, moderately, heavily, and severely polluted levels, respectively. More importantly, Kashgar had 16 (or 10) days with PM_{2.5} > 500 (or >1000) µg/m³. For Altay, the daily PM_{2.5} ranged from 4 to 44 µg/m³ in 2016. There were 308 days with PM_{2.5} ≤ 15 µg/m³, 362 days with PM_{2.5} ≤ 35 µg/m³, and only four days with PM_{2.5} of 35–75 µg/m³. Therefore, the AR of PM_{2.5} reached 100% for Altay, of which 362 days achieved the 24-h Grade I standard ($\leq 35 \mu\text{g}/\text{m}^3$), and all days during Apr to Sep met this standard.

3.2. Spatial autocorrelation analysis of PM_{2.5}

3.2.1. Global spatial autocorrelation analysis of PM_{2.5}

According to Eqs. (1) and (2), the Global Moran's I and Z-value for PM_{2.5} were calculated using ArcGIS 10.2 and GeoDa software. Spatial autocorrelation depends mostly on the Z-scores, which tell a researcher where features with either high or low values cluster spatially. Moran's I exceeded 0.45 in all the months of 2016 and reached 0.69 for annual PM_{2.5}, which demonstrates that a positive spatial autocorrelation exists for PM_{2.5} in China (Table 2). Monthly Moran's I was highest in Jan and was lowest in Aug. As for the Z-value, it was >13 and passed the significance test ($p < 0.001$) in all months, and was 19.93 throughout the year, implying that PM_{2.5} had significant spatial clustering characteristics.

Table 2

Results of spatial autocorrelation and hot spot analysis of PM_{2.5} (particles with an aerodynamic diameters $\leq 2.5 \mu\text{m}$) concentrations in 2016.

Period	Moran's I	Z-value	Hot spot			Cold spot		
			NH	99%	95%	NC	99%	95%
Jan	0.73	20.71	65	47	18	62	12	50
Feb	0.59	17.12	48	28	20	37	8	29
Mar	0.55	19.39	18	5	13	13	1	12
Apr	0.65	18.59	48	43	5	24	8	16
May	0.64	19.58	17	6	11	13	1	12
Jun	0.57	16.33	53	36	17	57	17	40
Jul	0.59	17.19	44	34	10	40	12	28
Aug	0.46	13.22	57	25	32	38	17	21
Sep	0.65	18.57	80	51	29	59	23	36
Oct	0.54	15.64	36	25	11	30	9	21
Nov	0.68	19.47	56	43	13	49	20	29
Dec	0.69	20.29	62	46	16	48	19	29
Annual	0.69	19.93	54	44	10	44	18	26

Note: NH and NC indicate the number of hot and cold spots with confidence level > 95%, respectively; 95% and 99% indicate the number of hot (or cold) spots identified at the 95% and 99% confidence level, respectively.

Specifically, cities with high or low PM_{2.5} were normally adjacent to cities with high or low PM_{2.5} (positive high-high correlation or positive low-low correlation), respectively. The highest clustering intensity (the maximal Moran's I) was found in Jan and the lowest (the minimal Moran's I) was observed in Aug.

3.2.2. Hot spot analysis of PM_{2.5}

In terms of Z(I), the rank of its value was Jan > Dec > May > Nov > Mar > Apr > Sep > Jul > Feb > Jun > Oct > Aug (Table 2), indicating strong and weak HS clustering occurred in Jan and in Aug, respectively (Fig. 4). Generally, the number of HSs with confidence levels (hereinafter "CL") >95% shows the extent of the areas influenced by PM_{2.5} pollution in this region. Eighty HS cities had CL >95% and HS was the most widely distributed in Sep, and was mainly concentrated in the North China Plain and central China, including Tianjin, Hebei, Shandong, Shaanxi, Henan, Chongqing, Hubei, and Hunan (Fig. 4, Table 2), of which 51 cities exceeded the 99% CL. The number of the HS cities with CL >95% was lowest in Mar and May; these cities with CL >99% were all in Xinjiang. The HS cities with CL >99% were mainly located in the BTH region and nearby southern and western regions in Jan, Aug, Nov, and Dec, while only a few with CL >95% were located in Xinjiang. In addition, the HS cities with CL >95% were distributed in both Xinjiang and the BTH region and nearby southern regions in Feb, Apr, Jun, Jul and Oct. The number of the CS cities with CL >95% peaked in Jan, and was lowest in Mar and May; those with CL >99% were greatest in number in Sep. Thus, the number of both HS and CS cities with CL >99% was largest in Sep, while the number of both HS and CS cities with CL >95% was smallest in Mar and May.

Aug and Sep are apparently different from the other months in terms of the distribution of HS areas (Fig. 4). HS (or CS) areas were areas with a spatial clustering of high (or low) values, but the high and low values were relative and not absolute. Although the monthly mean PM_{2.5} fell between 4.97 and 63.19 µg/m³ for 338 cities with an average of 28.16 ± 13.08 µg/m³ in Aug, the areas with relatively high PM_{2.5} (35–63 µg/m³) become larger and expanded to central China (Fig. 5). In Sep, the lowest and highest PM_{2.5} were 6.13 and 81.20 µg/m³, respectively, and the average PM_{2.5} was 35.17 ± 14.02 µg/m³; relatively high PM_{2.5} areas were concentrated in the range of 40–81 µg/m³ and these were also widely distributed. For comparison, the distribution of PM_{2.5} in Dec is also presented in Fig. 5; although PM_{2.5} (peaking at 252.10 µg/m³ and with an average of 76.60 µg/m³) was significantly greater than that in Aug and Sep, the cities with relatively high PM_{2.5} (115–252 µg/m³) were concentrated in smaller areas.

For annual distribution, 54 HS cities had a CL >95%, of which 44 cities exceeded the 99% CL; meanwhile, 44 CS cities had a CL >95%. Among the HS cities, five, seven, six, 12, three, two, 16, and one cities were in Xinjiang, central-south Hebei, central-south Shanxi, central-west Shandong, north Anhui, central Shaanxi plain, Henan, and northwest Jiangsu, respectively, in addition to Beijing and Tianjin (Fig. 4). In addition, seven provincial capital cities, Beijing, Tianjin, Shijiazhuang, Jinan, Zhengzhou, Xi'an, and Urumqi were in the rank of the HS. The CS cities were mainly distributed in southwest China, with several in northeast China and along the southeast coast of China.

4. Discussion

PM_{2.5} concentrations presented significant spatial clustering; HSs and heavy PM_{2.5} pollution were concentrated in southwest Xinjiang and in the BTH and neighboring regions.

The BTH and its surrounding regions are infamous for their serious air pollution problems (Cai et al., 2017). This region has the highest density of coal-based industries in China, such as coal-fired power plants, iron and steel plants, and cement industries, which are known as high-emission and high-pollution industries (Zhang and Cao, 2015). The enhanced PM_{2.5} pollution in this region has mainly been ascribed to the primary emissions coming from local sources (Zhao et al.,

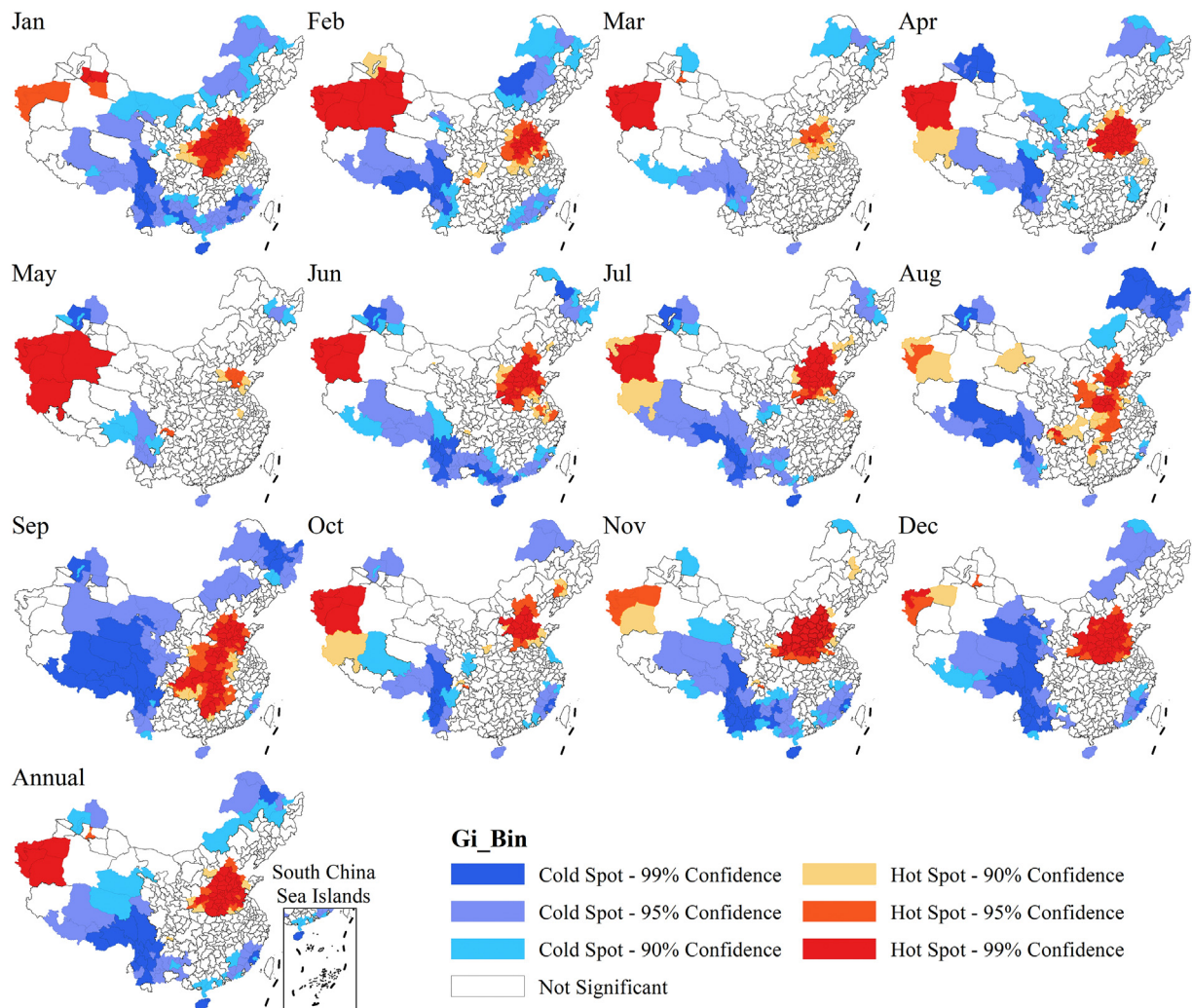


Fig. 4. The spatial distribution of hot and cold spots of monthly and annual PM_{2.5} (particles with an aerodynamic diameters $\leq 2.5 \mu\text{m}$) for 338 cities in 2016.

2013). Fig. S3 illustrates the distribution of smoke and dust emissions produced by industrial and household sources in 2016. Hebei Province contributed the largest volume of smoke and dust emissions (125.68×10^4 ton), followed by Shandong (87.38×10^4 ton), Shanxi (68.15

$\times 10^4$ ton), and Liaoning provinces (64.91×10^4 ton) (NBS, 2017). That is, these top four provinces are all located in the BTH and the surrounding areas, which led to high PM_{2.5} concentrations here. In addition, the influence of traffic emissions cannot be overlooked. Henan,

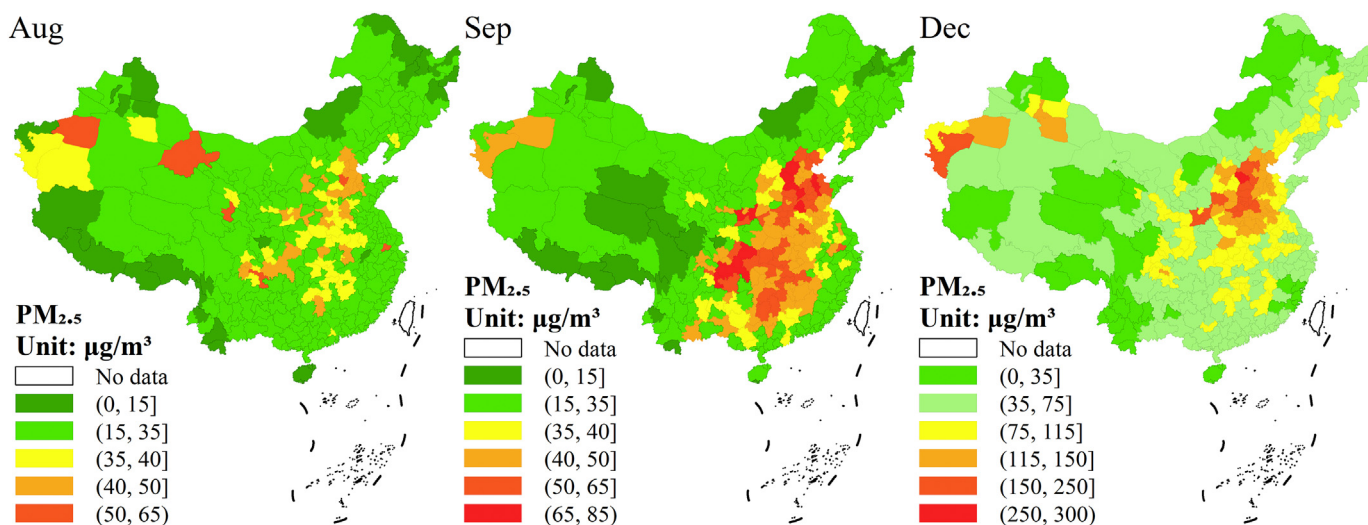


Fig. 5. Distribution of PM_{2.5} (particles with an aerodynamic diameters $\leq 2.5 \mu\text{m}$) in Aug, Sep and Dec of 2016.

Hebei, and Shandong recorded the highest emissions of particulate matter from vehicle exhaust at approximately 4.8×10^4 , 4.2×10^4 , and 3.8×10^4 tons in 2016, respectively (MEP, 2017a). Vehicle exhaust is an important PM_{2.5} source in the BTH region, especially in autumn and winter, a time when heavy and severe pollution occurs, and contributes approximately 30% to PM_{2.5} in Beijing, 20% in Baoding, and 15% in Shijiazhuang (Gao et al., 2016; MEP, 2017a; Ziková et al., 2016). What's more, regional transport of air pollutants and the formation of secondary pollution also have an important contribution to high PM_{2.5} in the BTH, especially for Beijing (Huang et al., 2014). Zhao et al. (2013) investigated the chemical composition of PM_{2.5} in the BTH region and found that the concentration of secondary inorganic ions was high in summer due to stronger photochemical oxidation, the concentration of secondary organic carbon (SOC) was high in autumn and winter, and SOC has greater percentages of increase than that of primary organic carbon during winter. Lang et al. (2017) and Ma et al. (2017) also reported that the proportion of secondary inorganic aerosols in PM_{2.5} increased and became the major components of PM_{2.5} in Beijing. Liu et al. (2014) pointed out that regionally transported aerosols contribute greatly (30.9%) to the PM_{2.5} concentration in Beijing. Another study showed that 25%–30% of the PM_{2.5} in Beijing comes from the contribution of surrounding areas in summer, while they contribute 32%–40% in winter (Xu, 2015).

However, the meteorological conditions of this region are often characterized by stagnant air masses that are favorable for the formation and accumulation of pollutants such as PM_{2.5}. Weak or low pressure leads to stable meteorological conditions with light winds, temperature inversions and low mixing layer heights. The inversion layer acts as a lid to prevent pollutants at ground level from dispersing, so that heavy pollution usually coincides with the occurrence of these inversions (Ji et al., 2012). As indicated by the China Climate Bulletin (CMD, 2016), stagnant air masses frequently occurred in the BTH in 2016, particularly in

wintertime. The frequency and severity of the related poor weather conditions here were higher than in other areas, which led to weak diffusion and reduced elimination of pollutants. In order to explore the effects of natural weather-related factors on PM_{2.5} concentrations, daily meteorological data, such as pressure, temperature, humidity, and wind speed were adopted to assess the relationship between weather and PM_{2.5} in the BTH and neighboring regions (Fig. 6). A significant relationship existed between daily PM_{2.5} concentrations and temperature, relative humidity, and wind speed, although no obvious relationships were found between PM_{2.5} and pressure. The decrease (or increase) in relative humidity can promote the decline (or rise) of PM_{2.5}. PM_{2.5} has a negative relationship with wind speed. That is, with increasing wind speed, PM_{2.5} showed a decreasing trend because high wind speed is helpful in dispersing PM_{2.5}. Temperature lower or higher than 0 °C were positively and negatively correlated with PM_{2.5}, respectively. Therefore, meteorological elements, including humidity, temperature, and wind speed, have a remarkable influence on PM_{2.5} concentrations in this region.

Southwest Xinjiang has become one of the most polluted areas of China and a new region where PM_{2.5} frequently exceeds the national standard in recent years (Li et al., 2017). Xinjiang ranked seventh (45.67×10^4 ton) and eleventh (2.2×10^4 ton) in China in 2016 in terms of industrial smoke and dust emissions as well as vehicle emission, respectively (MEP, 2017a; NBS, 2017); this was significantly lower than that in the BTH region. Fig. 7 illustrates that no obvious relationship was found between PM_{2.5} concentrations and meteorological factors in southwest Xinjiang, indicating that PM_{2.5} here was less influenced by meteorological factors such as pressure, temperature, humidity, and wind. In fact, the Taklimakan Desert is one of main sand dust source areas in China; this desert is located in south Xinjiang and is the largest desert in China and the world's second largest shifting sand

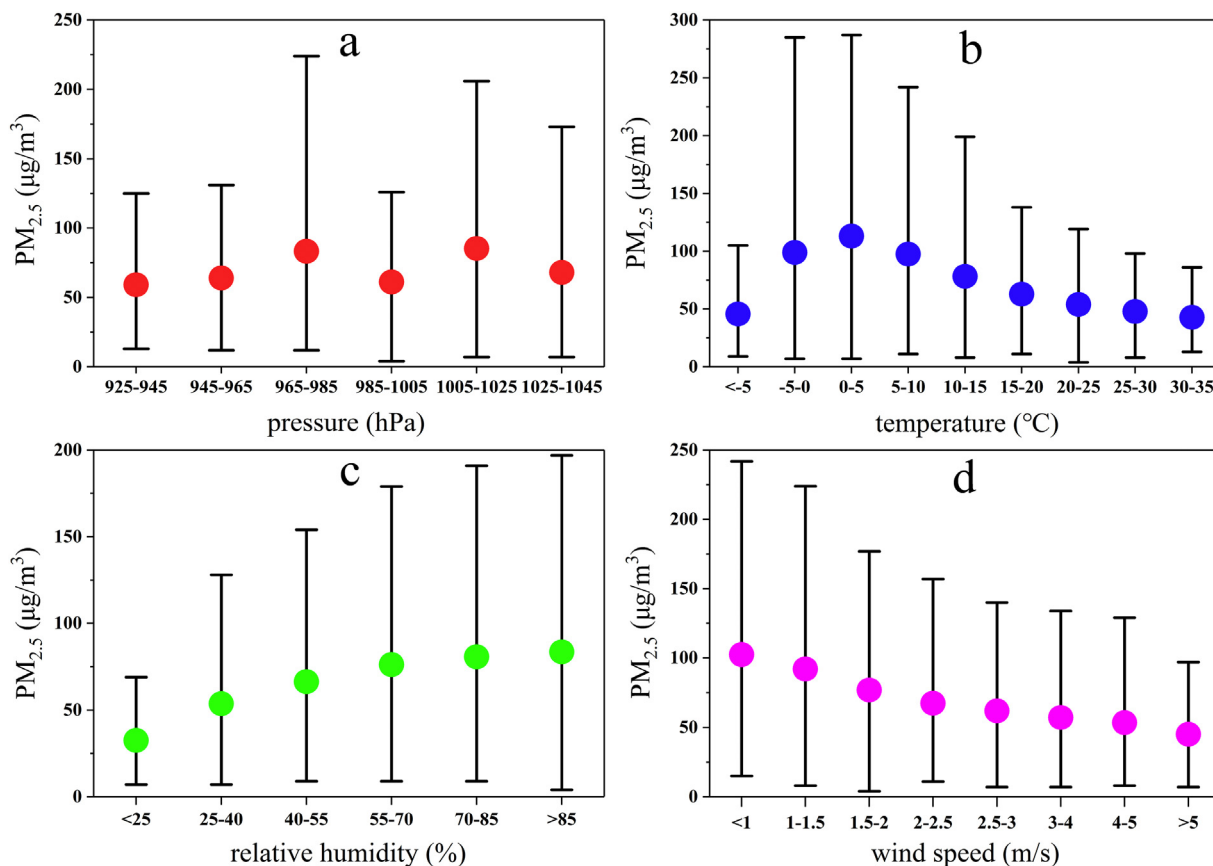


Fig. 6. Relationship between daily PM_{2.5} (particles with an aerodynamic diameters $\leq 2.5 \mu\text{m}$) concentrations and weather factors in the Beijing-Tianjin-Hebei region in 2016. Data source: China Meteorological Data Service Center (CMDC), <http://data.cma.cn/>.

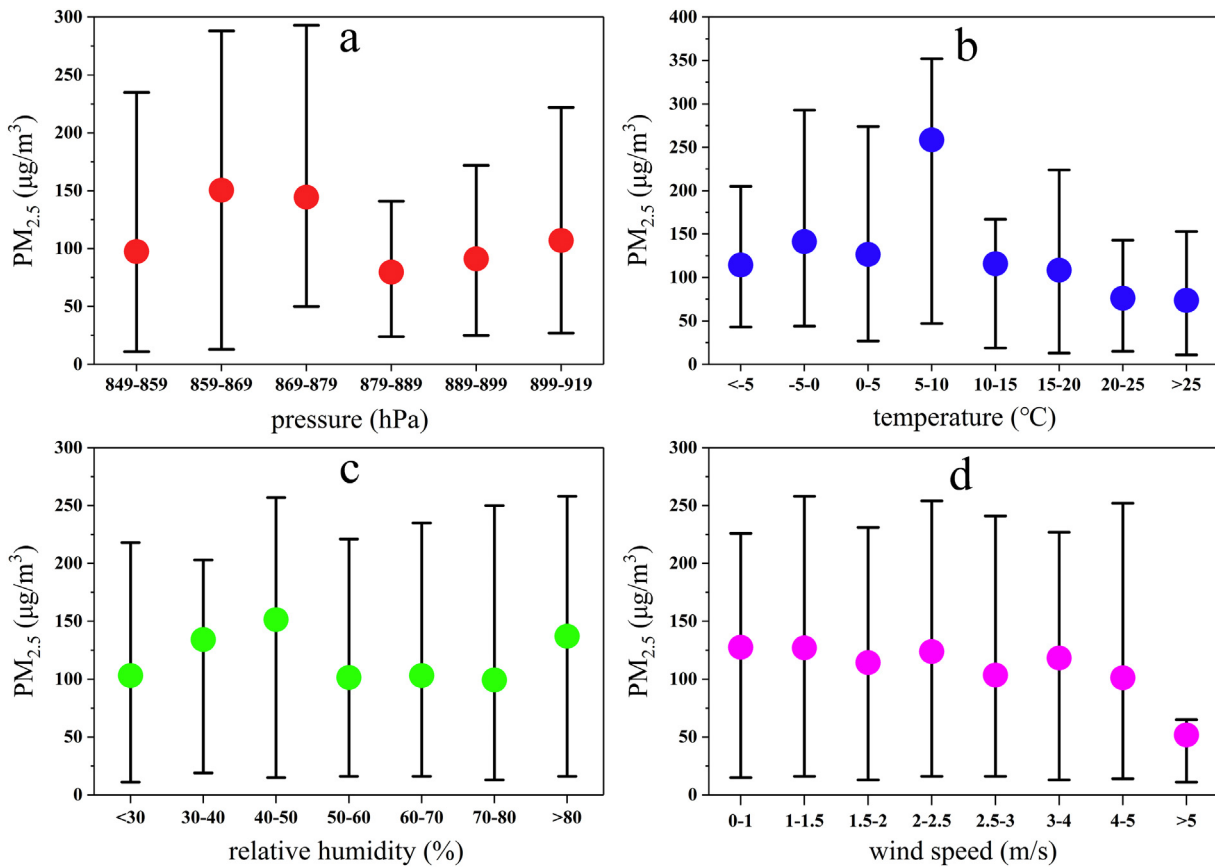


Fig. 7. Relationship between daily PM_{2.5} (particles with an aerodynamic diameters $\leq 2.5 \mu\text{m}$) concentrations and weather factors in southwest Xinjiang in 2016. Data source: China Meteorological Data Service Center (CMDC), <http://data.cma.cn/>.

desert, with about 85% of the desert area consisting of shifting sand dunes (Yang et al., 2012). The regional and local sandstorm events severely affect the PM_{2.5} concentrations in this region, especially in non-heating season. The regional sandstorms occur more frequently in spring, while localized sandstorms appear more frequently in summer (Ma et al., 2016). Local and regional sand-dust weather occurred 22 and 23 times, respectively, in 2016 (XJDEP, 2017), which led to a maximum monitored concentration of daily PM_{2.5} of 1771 $\mu\text{g}/\text{m}^3$ in Kashgar. In addition, coal-burning for domestic heating (from Oct to Mar of the next year) was another cause of PM_{2.5} pollution in this region; pollution from burning coal makes a large contribution to the heating season pollution (XJDEP, 2017).

With the influence of the above factors, southwest Xinjiang, as well as the BTH and its neighboring regions, were the two regions where heavy PM_{2.5} pollution occurred frequently, and these areas became the HSs of the spatial distribution of PM_{2.5} concentrations in China.

In terms of CSs, it implies that a city has low PM_{2.5} and is surrounded by cities with low PM_{2.5}. As mentioned above, CS cities were mainly in the southwestern and southern coastal areas of China. The CS here was not only attributed to the relatively lower emissions of particulate matter, including industrial and traffic sources in these areas (MEP, 2017a; NBS, 2017). The higher atmospheric mitigating capacity of the environment, which reflects the ability of the area to diffuse and eliminate pollution in the atmosphere, is a characteristic of this region compared with other areas, especially with the BTH region (CMD, 2016).

5. Conclusions

This paper used monitoring data of PM_{2.5} concentrations for 338 Chinese cities, revealing the spatial-temporal patterns and spatial

clustering of PM_{2.5} pollution based on statistical methods and exploratory spatial data analysis, and investigated the factors influencing PM_{2.5} concentrations. The results show that (1) annual mean PM_{2.5} falls between 10.28 and 157.01 $\mu\text{g}/\text{m}^3$ for all cities, with an average of $45.75 \pm 18.21 \mu\text{g}/\text{m}^3$ that exceeded the National Ambient Air Quality Standard of China. Only the annual PM_{2.5} levels of 103 (or four) cities met national Grade II (or Grade I) limit. PM_{2.5} was generally higher in the north than that in southern China. (2) Diurnal variations of PM_{2.5} showed a W-shaped tendency, with the lowest values were recorded in the afternoon around 16:00 each day. (3) The daily and monthly mean PM_{2.5} of all cities exhibited a U-shaped trend overall, while the attainment rate (the ratio of the number of cities attaining the national PM_{2.5} standards to all cities each day) presented an inverted U-shaped curve. Among the cities with daily PM_{2.5} over the standard, the largest proportion were classified as slightly polluted, with moderate and heavy pollution being fairly common at the beginning and end of the year. (4) A positive spatial autocorrelation for PM_{2.5} concentrations was observed when compared with high levels of Moran's I. (5) PM_{2.5} concentrations exhibited significant spatial clustering. Hot spots were concentrated in southwestern Xinjiang, along with the BTH region and adjoining western and southern regions, including Shanxi, Shandong, Hebei, Henan, and Anhui provinces. The cities with the highest annual PM_{2.5} and the lowest attainment rate were found in southwestern Xinjiang. (6) For the BTH region and surrounding areas, although meteorological factors can affect the variation of PM_{2.5}, the substantial emission of particulate matter in this region is the most direct and crucial factor. More measures, and measures that are stricter, need to be taken to control and reduce pollutant emissions. For southwest Xinjiang, the frequent occurrence of regional and local sandstorms contributes enormously to heavy PM_{2.5} concentrations, and weather factors have no obvious influence on PM_{2.5}.

Acknowledgements

This work is financially supported by the National Key R&D Program of China (No. 2016YFA0602601). The authors also gratefully acknowledge two anonymous reviewers for their constructive comments.

Appendix A. Supplementary data

Supplementary data to this article can be found online at <https://doi.org/10.1016/j.scitotenv.2018.03.057>.

References

- Anselin, L., 1988. *Spatial Econometrics: Methods and Models*. Kluwer Academic Publishers, Boston.
- Cai, S.Y., Wang, Y.J., Zhao, B., Wang, S.X., Chang, X., Hao, J.M., 2017. The impact of the “air pollution prevention and control action plan” on PM_{2.5} concentrations in Jing-Jin-Ji region during 2012–2020. *Sci. Total Environ.* 580, 197–209.
- Cao, J., Yang, C.X., Li, J.X., Chen, R.J., Chen, B.H., Gu, D.F., Kan, H.D., 2011. Association between long-term exposure to outdoor air pollution and mortality in China: a cohort study. *J. Hazard. Mater.* 186, 1594–1600.
- Chen, L., Shi, M.S., Gao, S., Li, S.H., Mao, J., Zhang, H.L., Sun, Y.L., Bai, Z.P., Wang, Z.L., 2017. Assessment of population exposure to PM_{2.5} for mortality in China and its public health benefit based on BenMAP. *Environ. Pollut.* 221, 311–317.
- CMD, 2016. China Climate Bulletin 2016. China Meteorological Administration (CMD), Beijing, China.
- Ding, L., Zhu, D.J., Peng, D.H., Zhao, Y., 2017. Air pollution and asthma attacks in children: a case-crossover analysis in the city of Chongqing, China. *Environ. Pollut.* 220, 348–353.
- Duan, Z., Han, X., Bai, Z.N., Yuan, Y.D., 2016. Fine particulate air pollution and hospitalization for pneumonia: a case-crossover study in Shijiazhuang, China. *Air Qual. Atmos. Health* 9, 723–733.
- Fontes, T., Li, P.L., Barros, N., Zhao, P.J., 2017. Trends of PM_{2.5} concentrations in China: a long term approach. *J. Environ. Manag.* 196, 719–732.
- Gan, M.L., Lv, W.Y., Fu, L., 2016. Spatial statistical analysis on PM_{2.5} in Chengdu based on improved Moran's I. *Environ. Sci. Technol.* 39, 187–193.
- Gao, J., Peng, X., Chen, G., Xu, J., Shi, G.L., Zhang, Y.C., Feng, Y.C., 2016. Insights into the chemical characterization and sources of PM_{2.5} in Beijing at a 1-h time resolution. *Sci. Total Environ.* 542, 162–171.
- Getis, A., Ord, J.K., 1992. The analysis of spatial association by the use of distance statistics. *Geogr. Anal.* 24, 189–206.
- Guo, Y.M., Jia, Y.P., Pan, X.C., Liu, L.Q., Wichmann, H.E., 2009. The association between fine particulate air pollution and hospital emergency room visits for cardiovascular diseases in Beijing, China. *Sci. Total Environ.* 407, 4826–4830.
- Haining, R.P., 1990. *Spatial Data Analysis in the Social and Environmental Sciences*. Cambridge University Press, Cambridge.
- Hao, Y.H., Zhang, G.H., Han, B., Xu, X.W., Feng, N.N., Li, Y., Wang, W., Kan, H.D., Bai, Z.P., Zhu, Y.L., Au, W., Xia, Z.L., 2017. Prospective evaluation of respiratory health benefits from reduced exposure to airborne particulate matter. *Int. J. Environ. Health Res.* 27, 126–135.
- Hu, M.G., Jia, L., Wang, J.F., Pan, Y.P., 2013. Spatial and temporal characteristics of particulate matter in Beijing, China using the empirical mode decomposition method. *Sci. Total Environ.* 458–460, 70–80.
- Hu, J.L., Wang, Y.G., Ying, Q., Zhang, H.L., 2014. Spatial and temporal variability of PM_{2.5} and PM10 over the North China plain and the Yangtze River Delta, China. *Atmos. Environ.* 95, 598–609.
- Huang, R.J., Zhang, Y.L., Bozzetti, C., Ho, K.F., Cao, J.J., Han, Y.M., Daellenbach, K.R., Slowik, J.G., Platt, S.M., Canonaco, F., Zotter, P., Wolf, R., Pieber, S.M., Bruns, E.A., Crippa, M., Cairelli, G., Piazzalunga, A., Schwikowski, M., Abbaspazade, G., Schnelle-Kreis, J., Zimmermann, R., An, Z.S., Szidat, S., Baltensperger, U., El Haddad, I., Prévôt, A.S.H., 2014. High secondary aerosol contribution to particulate pollution during haze events in China. *Nature* 514, 218–222.
- Ji, D.S., Wang, Y.S., Wang, L.L., Chen, L.F., Hu, B., Tang, G.Q., Xin, J.Y., Song, T., Wen, T.X., Sun, Y., Pan, Y.P., Liu, Z.R., 2012. Analysis of heavy pollution episodes in selected cities of northern China. *Atmos. Environ.* 50, 338–348.
- Jin, Q., Fang, X.Y., Wen, B., Shan, A.D., 2017. Spatio-temporal variations of PM_{2.5} emission in China from 2005 to 2014. *Chemosphere* 183, 429–436.
- Lang, J.L., Zhang, Y.Y., Zhou, Y., Cheng, S.Y., Chen, D.S., Guo, X.R., Chen, S., Li, X.X., Xing, X.F., Wang, H.Y., 2017. Trends of PM_{2.5} and chemical composition in Beijing, 2000–2015. *Aerosol Air Qual. Res.* 17, 412–425.
- Li, M.N., Zhang, L.L., 2014. Haze in China: current and future challenges. *Environ. Pollut.* 189, 85–86.
- Li, M.S., Ren, X.X., Yu, Y., Zhou, L., 2016. Spatiotemporal pattern of ground-level fine particulate matter (PM_{2.5}) pollution in mainland China. *China Environ. Sci.* 36, 641–650.
- Li, S.X., Zou, B., Liu, X.Q., Fang, X., 2017. Pollution status and spatio-temporal variations of PM_{2.5} in China during 2013–2015. *Research of Environ. Sci.* 30, 678–687.
- Liu, Z.R., Hu, B., Liu, Q., Sun, Y., Wang, Y.S., 2014. Source apportionment of urban fine particle number concentration during summertime in Beijing. *Atmos. Environ.* 96, 359–369.
- Liu, J., Hou, K.P., Wang, X.D., Yang, P., 2016. Temporal-spatial variations of concentrations of PM10 and PM_{2.5} in ambient air. *Pol. J. Environ. Stud.* 25, 2435–2444.
- Lu, F., Xu, D.Q., Cheng, Y.B., Dong, S.X., Guo, C., Jiang, X., Zheng, X.Y., 2015. Systematic review and meta-analysis of the adverse health effects of ambient PM_{2.5} and PM10 pollution in the Chinese population. *Environ. Res.* 136, 196–204.
- Ma, L.M., Zhang, X., 2014. A spatial econometric approach to studying regional air pollution in China. *Chin. Econ.* 9, 42–56.
- Ma, Z.W., Hu, X.F., Huang, L., Bi, J., Liu, Y., 2014. Estimating ground-level PM_{2.5} in China using satellite remote sensing. *Environ. Sci. Technol.* 48, 7436–7444.
- Ma, J.Y., He, Q., Yang, X.H., Huo, W., Yang, F., 2016. Characteristics analysis of regional and local sandstorm over the hinterland of Taklimakan Desert: taking Tazhong as example. *Desert Oasis Meteorol.* 10, 36–42.
- Ma, Q.X., Wu, Y.F., Tao, J., Xia, Y.J., Liu, X.Y., Zhang, D.Z., Han, Z.W., Zhang, X.L., Zhang, R.J., 2017. Variations of chemical composition and source apportionment of PM_{2.5} during winter haze episodes in Beijing. *Aerosol Air Qual. Res.* 17, 2791–2803.
- Mardones, C., Sanhueza, L., 2015. Tradable permit system for PM_{2.5} emissions from residential and industrial sources. *J. Environ. Manag.* 157, 326–331.
- MEP, 2012. Technical Regulation on Ambient Air Quality Index (on Trial). The Ministry of Environmental Protection (MEP), Beijing, China.
- MEP, 2013a. Technical Specifications for Installation and Acceptance of Ambient Air Quality Continuous Automated Monitoring System for PM₁₀ and PM_{2.5}. Ministry of Environmental Protection, Beijing, China, p. 25.
- MEP, 2013b. Technical Specifications for Installation and Acceptance of Ambient Air Quality Continuous Automated Monitoring System for SO₂, NO₂, O₃ and CO. Ministry of Environmental Protection, Beijing, China, p. 27.
- MEP, 2017a. China Vehicle Environmental Management Annual Report. Ministry of Environmental Protection (MEP), Beijing, China, p. 2017.
- MEP, 2017b. Report on the State of the Environment in China 2016. Ministry of Environmental Protection (MEP), Beijing, China, p. 61.
- Moran, P.A.P., 1948. The interpretation of statistical maps. *J. R. Stat. Soc. Ser. B Methodol.* 10, 243–251.
- NBS (National Bureau of Statistics of China), 2017. *China Statistical Yearbook-2017*. China Statistics Press, Beijing, China.
- Ord, J.K., Getis, A., 1995. Local spatial autocorrelation statistics: distributional issues and an application. *Geogr. Anal.* 27, 286–306.
- Peng, J., Chen, S., Lü, H.L., Liu, Y.X., Wu, J.S., 2016. Spatiotemporal patterns of remotely sensed PM_{2.5} concentration in China from 1999 to 2011. *Remote Sens. Environ.* 174, 109–121.
- Wang, Z.B., Fang, C.L., 2016. Spatial-temporal characteristics and determinants of PM_{2.5} in the Bohai rim urban agglomeration. *Chemosphere* 148, 148–162.
- Wang, Y.G., Ying, Q., Hu, J.L., Zhang, H.L., 2014. Spatial and temporal variations of six criteria air pollutants in 31 provincial capital cities in China during 2013–2014. *Environ. Int.* 73, 413–422.
- Wang, Z.S., Li, Y.T., Chen, T., Zhang, D.W., Sun, F., Pan, L.B., 2015. Spatial-temporal characteristics of PM_{2.5} in Beijing in 2013. *Acta Geograph. Sin.* 70, 110–120.
- Wang, S.J., Zhou, C.S., Wang, Z.B., Feng, K.S., Hubacek, K., 2017. The characteristics and drivers of fine particulate matter (PM_{2.5}) distribution in China. *J. Clean. Prod.* 142, 1800–1809.
- XJDEP, 2017. *Xinjiang Environmental Bulletin 2016*. Xinjiang Department of Environmental Protection, Urumqi, Xinjiang, China.
- Xu, T.T., 2015. Characteristics and Sources of Fine Particulate Matter Pollution in Typical Areas of North China. Beijing University of Technology, Beijing, China.
- Xu, W.J., He, F.F., Li, H.X., Zhong, L.J., 2014. Spatial and temporal variations of PM_{2.5} in the Pearl River Delta. *Res. Environ. Sci.* 27, 951–957.
- Xu, L.Z., Batterman, S., Chen, F., Li, J.B., Zhong, X.F., Feng, Y.J., Rao, Q.H., Chen, F., 2017. Spatiotemporal characteristics of PM_{2.5} and PM10 at urban and corresponding background sites in 23 cities in China. *Sci. Total Environ.* 599–600, 2074–2084.
- Yang, Y., Wang, J., Tian, M.Z., Chen, X.Q., 2012. Distribution characteristics and research method of sandstorms in China: a review. *J. Desert Res.* 32, 465–472.
- Yin, S., Wang, X.F., Xiao, Y., Tani, H., Zhong, G.S., Sun, Z.Y., 2017. Study on spatial distribution of crop residue burning and PM_{2.5} change in China. *Environ. Pollut.* 220, 204–221.
- Zhang, Y.L., Cao, F., 2015. Fine particulate matter (PM_{2.5}) in China at a city level. *Sci. Rep.* 5, 14884.
- Zhao, P.S., Dong, F., He, D., Zhao, X.J., Zhang, X.L., Zhang, W.Z., Yao, Q., Liu, H.Y., 2013. Characteristics of concentrations and chemical compositions for PM_{2.5} in the region of Beijing, Tianjin, and Hebei, China. *Atmos. Chem. Phys.* 13, 4631–4644.
- Zhou, L., Wu, J.J., Jia, R.J., Liang, L., Zhang, F.Y., Ni, Y., Liu, M., 2016. Investigation of temporal-spatial characteristics and underlying risk factors PM_{2.5} pollution in Beijing-Tianjin-Hebei area. *Res. Environ. Sci.* 29, 483–493.
- Zíková, N., Wang, Y.G., Yang, F.M., Li, X.H., Tian, M., Hopke, P.K., 2016. On the source contribution to Beijing PM_{2.5} concentrations. *Atmos. Environ.* 134, 84–95.